# Spatially Resolved Temperature Determination of an Air/Acetylene Flame Using the Two-Step Laser-Enhanced Ionization Technique

**CHIN-BIN KE and KING-CHUEN LIN***

*Department of Chemistry, National Taiwan University, Taipei, Taiwan 106, and*
*Institute of Atomic and Molecular Sciences, Academia Sinica, Taipei, Taiwan 106, Republic of China*

**We have demonstrated a two-step laser-enhanced ionization (LEI) technique to be potentially useful in measuring a spatially resolved temperature in an atmospheric air/acetylene flame. As a complement to the existing optical methods, LEI detection shares the advantages of extremely high sensitivity and the capability of achieving a high spatial resolution, confined to the dual-beam intersection area of 1 mm × 1 mm. A theoretical model was developed to precisely extract the temperature information from the obtained two-step LEI signal. The physical parameters required in the experiment include simply the relative values of the LEI signals, associated with the fine-structure doublets of a selected thermometric species, and their corresponding laser energies. The subsequent treatment is also convenient without the need to know the absolute energy of the incident laser beam and to accurately calibrate the detection system. Al and Ga were selected as the thermometric species. The resultant radial and axial temperature mappings are consistent with each other and are also comparable with those reported by other optical methods.**

Index Headings: **Laser-enhanced ionization; Flame temperature determination.**

## INTRODUCTION

Flame temperature measurement has been an important subject in the field of combustion chemistry. Any chemical kinetics, thermal equilibrium, ionization, excitation, and other physical behavior in an analytical flame may be significantly characterized by its environmental temperature. Therefore, accurately diagnosing the temperature provides a basis for further understanding of these chemical and physical events and is also conducive to optimizing the combustion parameters in a flame.[1–3] For monitoring the flame temperature, a spectroscopic method provides a nonintrusive measurement, having the advantage of avoiding interference from combustion components. Two-line emission or absorption and line-reversal methods are conventionally used as the tools.[1–3] Laser-based techniques such as laser-induced fluorescence (LIF),[4–6] coherent anti-Stokes Raman scattering (CARS),[3,7] Rayleigh scattering, and degenerate four-wave mixing (DFWM) are commonly employed.[8–10] Most of these methods rely on the assumption of a local thermal equilibrium, in which the flame temperature is represented in terms of electronic, vibrational, rotational, and translational behavior of the seeded thermometric species.

The CARS technique is capable of achieving a high spatial and temporal resolution for a temperature mapping. However, it is limited by weak sensitivity, so that high number density of the thermometric species is required.[7] The LIF method offers better detection sensitivity, but sometimes suffers from collisional quenching and post-filter effects. Thus, a more complicated but careful manipulation is needed to extract the temperature information from the obtained signal. The DFWM method has been recently developed to measure rotational temperature. With the capability of detecting trace levels without suffering from interference from a flame background, this technique proves to be potentially useful for probing high spatial resolution of the temperature. As applied to thermometry, however, this method requires a critical understanding of the dependence of the scattering cross section on the rotational quantum number. Another problem, for instance, encountered by a broad-band DFWM approach arises from the narrowness of the laser spectral band. Thus only a few rotational lines can be covered in one laser shot, and the corresponding temperature may possibly include a large error.[8] As a complement to these optical methods, in this work, we demonstrate an alternative approach based on a two-step laser-enhanced ionization (LEI) technique. This kind of LEI detection proves to be capable of mapping flame temperatures with high spatial resolution and sensitivity.

Laser-enhanced ionization spectroscopy in flames has been successfully developed to detect trace metal concentrations at the sub-pg/mL level in aqueous solution with extremely high sensitivity and selectivity.[11–16] In addition, applications may include such tasks as measurement of the number density of free atoms released and, in turn, the atomization efficiency,[17] monitoring of ion lifetime,[18] determination of ion diffusion and mobility coefficients,[19,20] and resolution of spectral structures of atoms, molecules, and radicals.[21] The LEI technique can also be interfaced to flow injection to reduce matrix interference effects[22,23] and serve as a chromatographic detector.[24,25] As reported previously, by measuring ion mobility and diffusion coefficients of a thermometric species, one may determine the flame temperature on the basis of the Einstein relation.[20] The advantage of the LEI method lies in its capabilities of achieving high spatial resolution and avoiding optical interference from scattered radiation and flame background radiation. Nevertheless, one should assume that the size of the electrode as the ion collector is negligible and the electric field applied between them homogeneous. A precise measurement of ion diffusion and mobility coefficients is not trivial. An error propagation may lead to a large systematic error. Instead of using the Einstein relation, we have re-

Received 30 May 1997; accepted 27 August 1997.
* Author to whom correspondence should be sent.


0003-7028/98/5202-0187$2.00/0

cently developed a model to relate the measured LEI signals to the corresponding Boltzmann populations of the fine-structure doublets of the thermometric species, from which the electronic excitation temperature may be derived.[26] The feasibility and accuracy of the LEI temperature detection are found to be comparable to those of other optical methods. However, the temperature thus obtained is restricted to a spatial average along the laser beam directed through the slot burner.

In this work, we use stepwise excitation to enhance the LEI signal intensity, improving the detection sensitivity by up to two orders of magnitude. In addition, the configuration of the dual-laser beams is arranged in such a way that one beam intersects perpendicularly with the other one inside the flame. The temperature results for the interaction regime are confined to a very limited size. In this manner, the LEI method shares the advantages of extremely high sensitivity and capability of achieving a spatially resolved temperature, as in LIF and DFWM. We also developed a theoretical model, based on previous work,[26] to extract the temperature information from the measured two-step LEI signal. We measured radial and axial temperature profiles, with Al and Ga as the thermometric species, to demonstrate the reliability of this technique. A comparison with other optical methods will be discussed.

## EXPERIMENTAL

**Flame Burner.** The experimental apparatus of a two-step LEI has been illustrated previously,[11,15,16,26] so only a brief description is given below. We performed the LEI experiment, as shown in Fig. 1, by using a commercial burner assembly (Perkin-Elmer) with a 100 mm × 0.5 mm slot burner head, coupled with an interlocked gas control system by which acetylene (0.8 L/min) and air (13 L/min) were premixed prior to reaching the burner head.

**Reagent.** Al and Ga chloride salt were used as the reagents. Each aqueous salt solution was nebulized at a flow rate of 4.5 mL/min into the flame. The linearity of concentration dependence of the LEI signal has been carefully checked. Thus, the concentrations of 150 and 50 ppm (μg/mL) of Al and Ga salt solutions, which lay within the range of linearity, were prepared throughout the experiment of temperature determination.

**Dual-Beam Configuration.** In this work, two tunable dye lasers (Spectra-Physics PDL-2A and PDL-3), each pumped by individual Nd: YAG lasers (Spectra-Physics, DCR-2A and GCR-3), were used as radiation sources. One dye laser was operated so that the beam propagated longitudinally through the flame and intersected perpendicularly with the other one. The configuration is illustrated in Fig. 1b. The interaction position was moved successively along the lateral side with the use of a three-dimensional translational stage, equipped with micrometer, attached to the burner. The height from the burner top was adjusted from 2.5 ± 0.5 to 12.5 ± 0.5 mm. The two beams overlapped temporally and spatially inside the flame. The unfocused beams were collimated through an aperture 1.0 ± 0.5 mm in diameter to produce a homogeneous photon flux through the flame. In this manner, the scattered light was minimized, so that ionization of

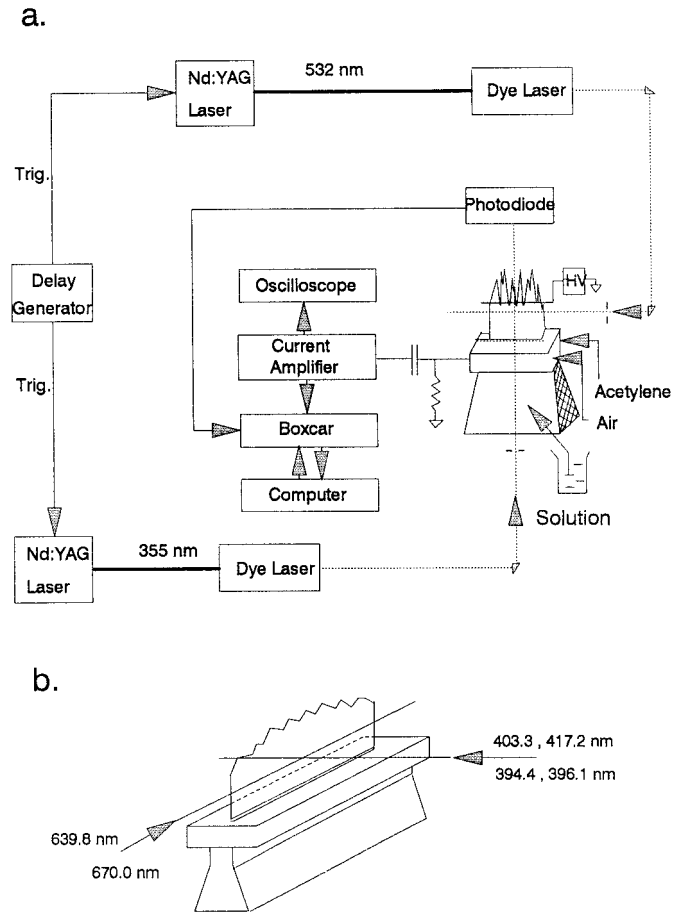


FIG. 1. (**a**) Schematic diagram of the experimental setup for the two-step LEI detection. (**b**) The configuration of dual laser beams directed towards the flame.

sample atoms caused by light scattering could be neglected.[27]

**Two-Step LEI Detection System.** The energy schemes of the two-step LEI process for Al and Ga are shown in Fig. 2. For the case of Al, the first laser was scanned over the wavelength range of 393–397 nm to select the atomic transitions from the fine-structure doublets to the $4^2S_{1/2}$ state, while the second laser was fixed at 670.0 nm in the $5^2P_{3/2} \leftarrow 4^2S_{1/2}$ transition. Analogously, for the case of Ga, the wavelength range of the first laser was scanned over 402–418 nm, while the second laser was fixed at 639.8 nm. As the wavelength of the first laser was resonant with the $^2S_{1/2} \leftarrow ^2P_{1/2,3/2}$ transitions, the stepwise excited atoms could be subsequently collisionally ionized. The resulting LEI ions were collected with a water-cooled cylinder probe along the flame, biased at −1000 V and suspended 1.5–2.0 cm above the burner head.[16] In an effort to avoid interference from flame components, the electrode was positioned slightly outside the flame, about 4–6 mm off the axis of the burner slot. The ion enhancement in this work proved to be comparable to that obtained with the electrode inside the flame. The burner served as the other electrode, from which the ion current was collected and amplified with a current-to-voltage converter (Keithley, Model 428), and then fed into a boxcar averager (PAR, Model 4402, 4420, and 4422) for signal processing. The result was displayed on

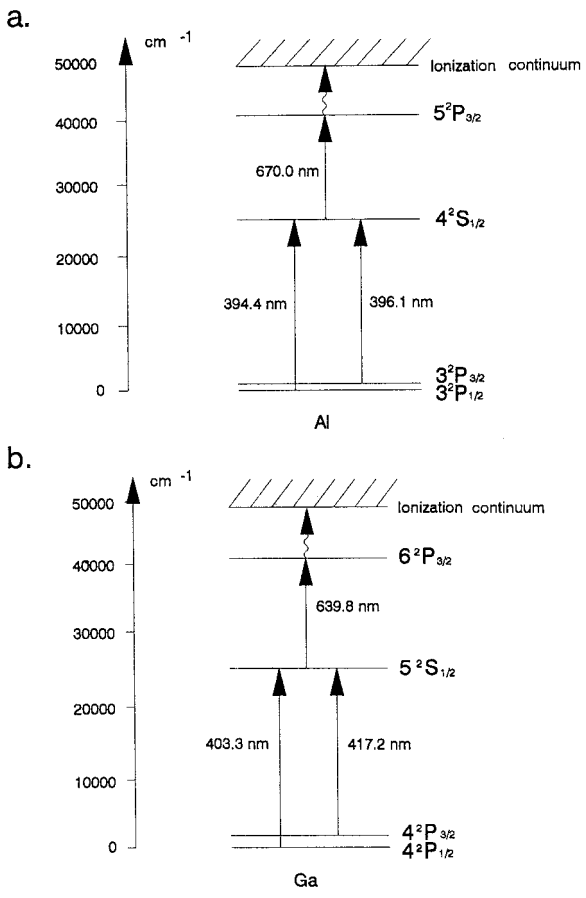


FIG. 2. Partial energy diagrams for the Al and Ga atoms.

an oscilloscope (Tektronix, Model 2445) or stored in a microcomputer for later data treatment. The corresponding laser energy for the first-step excitation was monitored simultaneously with either a photodiode (Hamamasu, s2386) or an energy meter (Scientech 36-0001).

## THEORETICAL MODELING

The theoretical modeling for the two-step LEI detection approach is based on our previous work with one-step LEI.[26] The essence of the model relies on the association of the temperature with a Boltzmann population difference between the ground and the excited fine-structure doublets of a selected species. The relationship between the observed ion signal and the state population affects the reliability and precision of the estimated temperature.

**One-Step LEI.** The energy schematic diagrams of single-step and two-step LEI are displayed in Fig. 3. The populations in the ground and excited fine-structure state, $l$ and $l'$, are excited alternatively to an intermediate state $u$, and then ionized via the collisional process. For the two-step LEI scheme, an additional photon promotes the population from the $u$ state to a higher $h$ state. In the LEI scheme, Omenetto et al.[13] and Travis[28] suggest that the ion yield is proportional to the product of the steady-state population density, $n_u$, of the excited state, and its collisional ionization rate coefficient, $K_{ui}$. Within the limit of the two-level approximation and with the assumption of

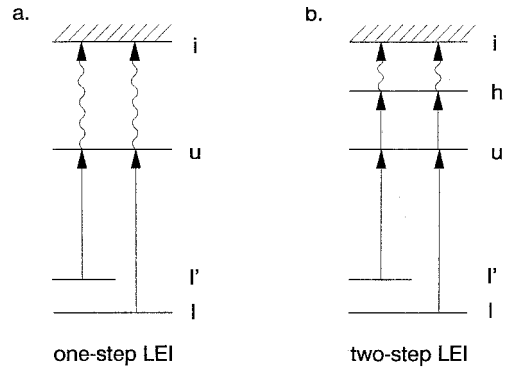


FIG. 3. Energy diagram employed in the theoretical model for (**a**) one-step LEI, and (**b**) two-step LEI.

a broad-band laser, the population density for $n_u$ and $n_l$ may be derived as

$$n_u = n_t g_u I_\lambda / (g_u + g_l)(I^s_\lambda + I_\lambda), \quad (1)$$

$$n_l = n_t((g_u + g_l)I^s_\lambda + I_\lambda)/(g_u + g_l)(I^s_\lambda + I_\lambda) \quad (2)$$

where $n_t$ denotes the total population density, equal to $n_u + n_l$; $g_u$ and $g_l$ are the statistical weight for the $u$ and $l$ state; $I_\lambda$ is the spectral irradiance; and $I^s_\lambda$ is its saturation parameter. If a relatively weak laser intensity, $I_\lambda \ll I^s_\lambda$, is assumed, and $n_l$ is close to its thermal population density $n_l^{th}$, then $n_u$ can be approximated by

$$n_u \approx n_l^{th}(g_u/g_l)I_\lambda \lambda_{ul}^5 A_{ul} \tau_u / (8\pi hc^2) \quad (3)$$

where $\tau_u$ is the lifetime of the upper state $u$; $A_{ul}$, the Einstein spontaneous emission coefficient from the $u$ to $l$ state; $\lambda_{ul}$, the emission wavelength from the $u$ to $l$ state; $c$, the light speed; and $h$, Planck's constant. If a fast collision redistribution among excited states lying between the state $u$ and the continuum state $i$ is assumed, then the ionization rate coefficient $K_{ui}$, due to collision, for the state $u$ may be given as[13]

$$K_{ui} = \bar{\nu}\sigma_u n_i \exp[-(E_i - E_u)/kT] \quad (4)$$

where $\sigma_u$ is the cross section for the colliding process; $\bar{\nu}$, the relative average velocity between the atom and the collider in the flame; $n_i$, the number density of the collision partner; $T$, the flame temperature; and $E_i$ and $E_u$, the energy of the continuum and the upper state, respectively. Thus the single-step LEI signal $S_{lu}$ from the ground fine-structure state $l$ can be described as

$$S_{lu} \propto n_l^{th}(g_u/g_l)I_\lambda \lambda_{ul}^5 A_{ul} \exp[-(E_i - E_u)/kT]. \quad (5)$$

Note that the values of $\bar{\nu}$, $\sigma_u$, $\tau_u$, and $n_i$ for the single-step LEI scheme initiated from either the $l$ or $l'$ state are the same; thus these parameters are omitted in Eq. 5 when comparing the LEI signals between $S_{lu}$ and $S_{l'u}$.

**Two-Step LEI.** The ion enhancement induced by a two-step LEI scheme is strongly affected by the second-step excitation. The explicit formula is expressed as[15]

$$S_{lh}(\text{TLEI}) = \frac{\lambda_{uh}^2 A_{hu} I_{uh} k_{hi}}{2\pi \Delta\omega_{uh} k_{ui}} S_{lu}(\text{SLEI}). \quad (6)$$

The ion enhancement of two-step LEI (TLEI) over single-step LEI (SLEI) may be attributed to such factors as second-step transition probability, laser intensity, colli-

sional ionization rate coefficients, and transition linewidth, which is associated with the effective lifetime of the states involved in the transition. Equation 6, ignoring the possibility of atom depletion during the laser pulse, is equivalent to equation 36 given by Axner et al.[29] The atom depletion effect may become negligible by an appropriate selection of the upper state $h$, so that the inverse of collisional ionization rate from this state is larger than the laser pulse duration.[15]

Provided that the laser energy and wavelength for the second-step excitation are fixed, the enhanced factor becomes constant. Analogously to Eq. 5, therefore, the TLEI signal can be expressed as

$$S_{lh}(\text{TLEI}) \propto F n_l^{\text{th}}(g_u/g_l) I_\lambda \lambda_{ul}^5 A_{ul} \exp[-(E_i - E_u)/kT]. \quad (7)$$

The proportional constant $F$ is the same for both TLEI signals associated with the $l$ and $l'$ states. The ratio of the thermal population density, $n_l^{\text{th}}$ and $n_{l'}^{\text{th}}$, for the ground and the excited fine-structure doublets follows the Boltzmann distribution. That is,

$$n_l^{\text{th}}/n_{l'}^{\text{th}} = (g_l/g_{l'})\exp[-(E_l - E_{l'})/kT]. \quad (8)$$

Asuming that the laser energy for the first-step excitation is weak, using the relations in Eqs. 7 and 8, we can derive the ratio of two-step LEI signals associated with the ground and the excited fine-structure doublets as

$$S_{lh}(\text{TLEI})/S_{l'h}(\text{TLEI}) = (I_\lambda/I'_\lambda)(\lambda_{ul}^5/\lambda_{ul'}^5)(A_{ul}/A_{ul'}) \exp[(E_{l'} - E_l)/kT]. \quad (9)$$

This equation is further rearranged to give an explicit, practical relation for the temperature measurement in this work as

$$T = (E_{l'} - E_l)/(kQ), \quad (10)$$

$$Q = \ln(S_{lh} I'_\lambda \lambda_{ul'}^5 A_{ul'}/S_{l'h} I_\lambda \lambda_{ul}^5 A_{ul}). \quad (11)$$

Given the spontaneous transition propabilities and the corresponding wavelengths for the pertinent atomic transitions, by measuring the LEI signal, one may determine the flame temperature using Eqs. 10 and 11. For an alternative excitation scheme, $l \rightarrow u$ and $l' \rightarrow u'$, in which the intermediate states $u$ and $u'$ are different, an analogous equation may also be derived. However, additional parameters involved may reduce the accuracy of the determined temperature.

## RESULTS AND DISCUSSION

**Excitation Temperature Determination by Al Species.** *LEI Spectra and Data Treatment.* In the case of Al, the first laser was scanned across the transitions of $4^2S_{1/2} \leftarrow 3^2P_{1/2,3/2}$, while the second laser was fixed at 670.0 nm. The resulting two-step LEI signal is shown in Fig. 4. If the laser at 670.0 nm was blocked, the single-step LEI was taken under otherwise identical condition. As shown in Fig. 4, one can hardly observe any single-step LEI signal for the Al atom. We could not detect any signal either, as a result of irradiation of the second laser alone at 670.0 nm. The lack of a detectable one-step LEI signal arises from the existence of a large ionization potential, which reduces the collisional ionization rate for the Al atom in the intermediate state. The other important reason is attributed to the fact that the detected total number of the species is restricted to a very small volume. The beam

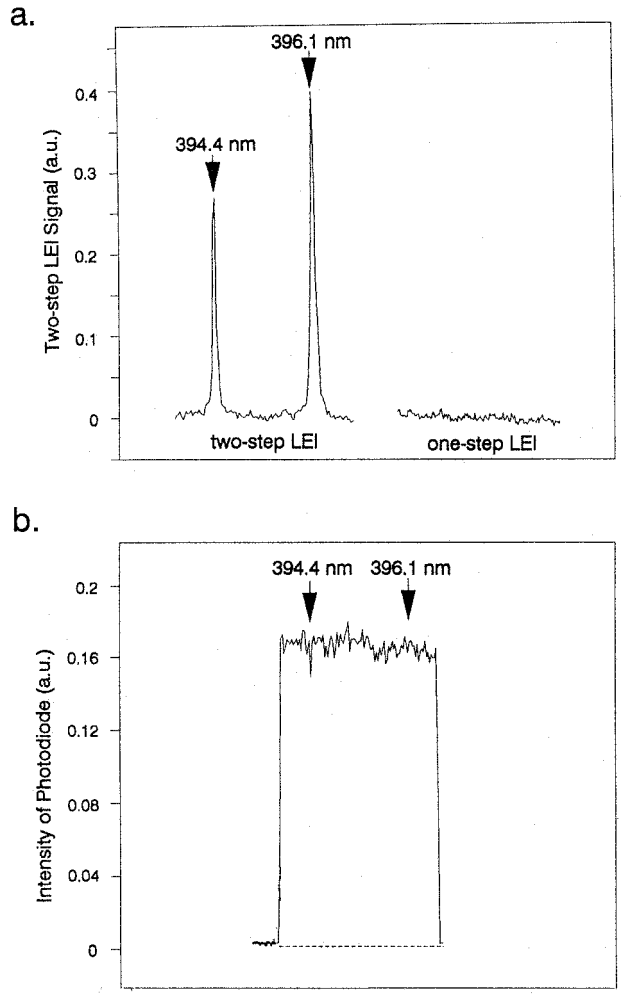


FIG. 4. (**a**) Two-step and one-step LEI spectra of 150 ppm Al. The former spectrum was obtained with irradiation of dual lasers simultaneously, while the latter was obtained without irradiation of the second laser at 670.0 nm. (**b**) The corresponding laser energy for the first-step excitation.

arrangement for the first laser is guided perpendicularly to the axis of the burner slot, unlike the conventional LEI alignment with the laser directed along the flame burner. The current LEI detection of Al provides a very clean and steady ion background, contributed by the single-laser ionization process alone. In this sense, the two-step LEI apparatus is operated like a null-detection device rather than a differential measurement technique. Thus the measured signal-to-noise ratio is greatly improved. In addition, the measured LEI signal results from the spatially overlapped region between dual beams, and the derived temperature corresponds to this limited area.

For the determination of a flame temperature, two physical parameters are required in the measurement. They are (1) the ratio of two-step LEI signals initiated between fine-structure doublets of the species selected, and (2) the ratio of corresponding laser energies used in the respective first-step excitation from these two doublets. The validity of Eqs. 10 and 11 requires the laser energy for the first-step excitation to be weak enough to be linear to the measured LEI signal. Figure 5 shows the energy dependence of the two-step LEI signals relevant to the $3^2P_{1/2}$ and $3^2P_{3/2}$ states, respectively. Due to a small energy separation of the fine-structure doublets, the cor-

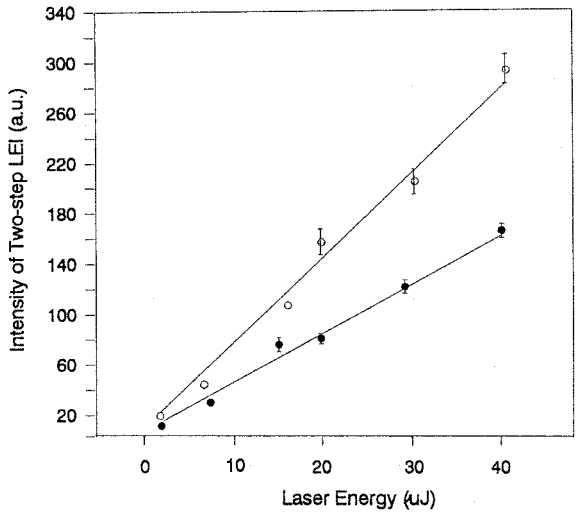


FIG. 5. Laser energy dependence of two-step LEI signals, associated with the atomic transitions at 394.4 nm (●) and 396.2 nm (○), respectively, from the ground and the excited fine-structure doublets of the Al atom. The concentration of Al was 150 ppm. The second laser at 670.0 nm was fixed at 150 μJ.

responding energies at these two transition wavelengths were almost the same (Fig. 4). The laser energy was measured with a photodiode, since there was no need to measure the absolute value. Whenever it is necessary, the exact energy may be readily measured with an energy meter instead. In this work, we kept the energy of the second laser at 150 μJ, which is linear in the region, as well. In fact, it is unnecessary, because Eqs. 10 and 11 are applicable to both conditions of optical saturation and unsaturation for the second-step laser.

*Temperature Profiles.* Given the slopes, $S_{lh}/I_\lambda$ and $S_{l'h}/I_\lambda$, the corresponding excitation wavelengths, and the spontaneous emission coefficients, the temperature may be evaluated. The related parameters are listed in Table I. The beam direction of the first laser was moved successively along the side of the flame; thereby the radial temperature profile, at 10 mm above the burner head, was obtained (Fig. 6a). The error bars were estimated for five replicates. The temperature varied from 2400 to 2550 K. The values in the central region appear to be 150 K higher than those near the edge. A cooler flame in the edge is readily interpreted as arising from intrusion of the ambient air. We also measured the axial-position dependence of the flame temperature by adjusting the height from 2.5 mm to 12.5 mm above the burner head. The result is shown in Fig. 6b, in which the radial position at 0 mm was measured. It is found that the temperature declines slightly from 2550 to 2500 K as the height is increased. The measured temperature profiles for both axial and radial distributions seem to be very steady without any dramatic changes.

*Spatial Resolution.* In this work, the spatial resolution of the flame temperature was confined within 1 mm × 1 mm, depending on the aperture through which the unfocused laser beam was directed. In theory, the spatial resolution may be improved to the micrometer level, if a focused beam is used for the first-step excitation. The slight difference in beam waists caused by different transition wavelengths for the doublets will not introduce much error in the evaluation of the $S_{lh}/I_\lambda$ value, if one is careful to measure the laser energy at the interactive position. The major problem to avoid arises from the fact that the focused beam of the first laser easily results in optical saturation, which will not meet the model condition.

**TABLE I. The relevant parameters associated with the first-step excitation for the Al and Ga species. The uncertainty for the spontaneous emission coefficient, A, is 25%.[43]**

| Element | Transition | λ (nm) | Dye | A($10^8$ $s^{-1}$) |
|---|---|---|---|---|
| Al | $3^2P_{1/2} \rightarrow 4^2S_{1/2}$ | 394.4 | LD390 + Stilbene 420[a] | 0.493 |
| | $3^2P_{3/2} \rightarrow 4^2S_{1/2}$ | 396.2 | LD390 + Stilbene 420[a] | 0.98 |
| | $4^2S_{1/2} \rightarrow 4^2P_{3/2}$ | 670.0 | DCM + LDS688[b] | |
| Ga | $4^2P_{1/2} \rightarrow 5^2S_{1/2}$ | 403.3 | LD390 + Stilbene 420[a] | 0.49 |
| | $4^2P_{3/2} \rightarrow 5^2S_{1/2}$ | 417.2 | LD390 + Stilbene 420[a] | 0.92 |
| | $5^2S_{1/2} \rightarrow 5^2P_{3/2}$ | 639.8 | DCM | |

[a] LD390 : Stilbene 420 was mixed in a volume ratio of 2:1.
[b] DCM : LDS698 was mixed in a volume ratio of 1:1.

**Temperature Determination by Ga Species.** The energy difference between the fine-structure doublets of Al is 112 $cm^{-1}$. The small energy separation does not allow for very accurate temperature determination. Therefore, we select the other thermometric species of Ga, with an energy separation of 827 $cm^{-1}$ between the doublets, to

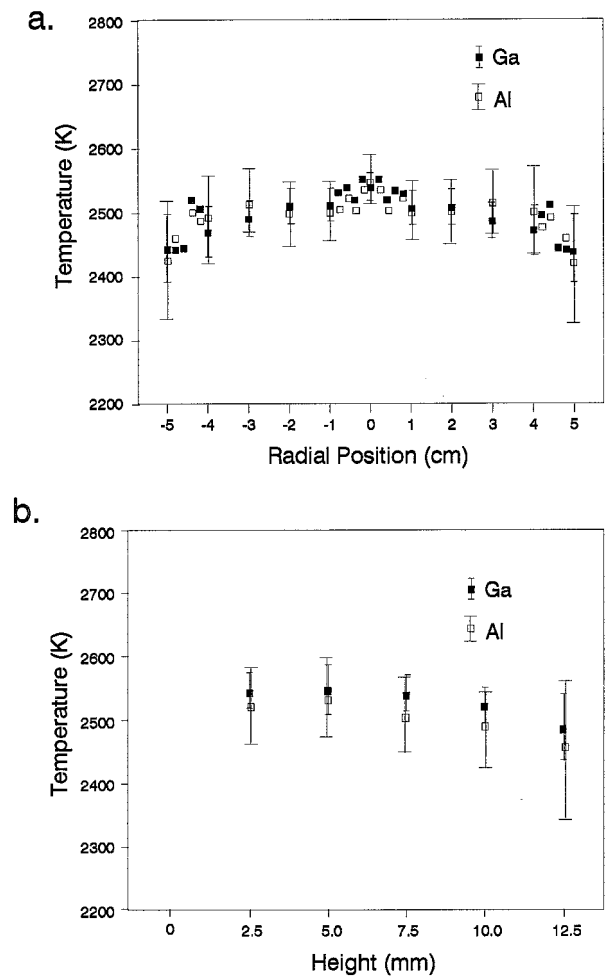


FIG. 6. (**a**) Radial temperature profile, measured at a height 10 mm from the burner top. (**b**) Axial temperature profile, measured at the central burner.

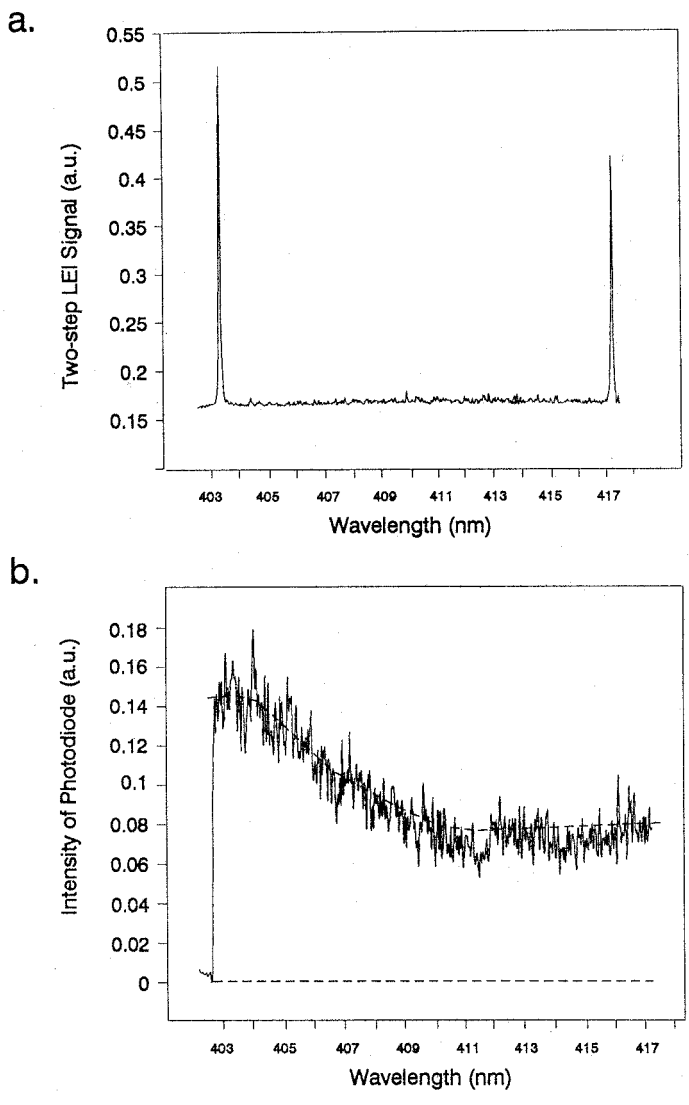


FIG. 7. (**a**) Two-step LEI spectra of 50 ppm Ga, of which one laser is scanned across the atomic transition $5^2S_{1/2} \leftarrow 4^2P_{1/2,3/2}$ while the other laser is fixed at 639.8 nm. (**b**) The corresponding laser energy for the first-step excitation, detected with a photodiode.

confirm reliability with the two-step LEI model. The wavelength of the first laser was scanned across the atomic transitions $5^2S_{1/2} \leftarrow 4^2P_{1/2,3/2}$, while the second laser was fixed at 639.8 nm. The resultant LEI signal is shown in Fig. 7, which was probed in the central position, 10 mm above the burner head. The figure also displays the corresponding energy of the first laser, as measured with a photodiode. Its radiant sensitivity at a wavelength of 417 nm was reported to be 7% larger than that at 403.3 nm. The corrected energy dependence of the two-step LEI signals, initiated from either the $4^2P_{1/2}$ or the $4^2P_{3/2}$ state, exhibits a relation of linear proportion, as shown in Fig. 8. The condition of the second laser at 639.8 nm was kept at 120 μJ, which was controlled to be unsaturated, although it was not necessary. Substituting the measured slopes and the relavent parameters into Eqs. 10 and 11, one may determine the spatially resolved flame temperature. By analogy with the Al case, the flame temperature was measured axially and radially, as shown in Fig. 6. Each error bar was estimated for five replicates. The distribution of the temperature profile is consistent with the case obtained with Al.

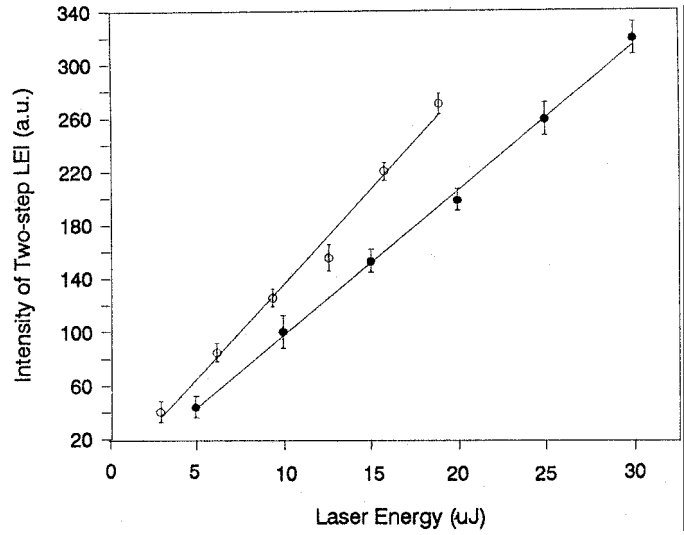


FIG. 8. Laser energy dependence of two-step LEI signals, associated with the atomic transitions at 403 nm (●) and 417 nm (○), respectively, from the ground and the excited fine-structure doublets of the Ga atom. The concentration of Ga was 50 ppm. The second laser at 639.8 nm was fixed at 120 μJ.

The temperature uncertainty $\Delta T$ can be evaluated according to Eq. 12:

$$\frac{\Delta T}{T} = \frac{kT}{E_{l'} - E_l}\sqrt{\left(\frac{\Delta S}{S}\right)^2 + \left(\frac{\Delta I}{I}\right)^2} \qquad (12)$$

where $k$ is the Boltzmann constant; $S$ and $I$ denote the measured LEI signal and the corresponding laser energy. $\Delta T$ is reciprocally proportional to the energy difference $E_{l'} - E_l$. The use of Ga as the thermometric species to replace Al may theoretically improve the temperature precision by a factor of 8. While considering the standard deviations of the measured LEI signal and the laser energy, we find that Ga yields a temperature precision two times better than Al (Fig. 6).

**Comparison with Other Optical Methods.** *Advantages of Two-step LEI.* As compared with the old versions of LEI temperature detection,[20,26] this study has several advantages. First, the new method provides a feasible and convenient way to carry out the experiment. The temperature determination relies on a straightforward measurement of the relative values of the LEI signals and the corresponding excitation energy associated with the fine-structure doublets. There is no need to calibrate the detection system and to monitor the absolute energy of the incident laser. Second, this work is capable of achieving a high spatial resolution. Third, a two-step LEI is used instead, improving markedly the sensitivity to the species detection. In the cases of Ga and Al, for instance, the ion enhancement of two-step LEI over single-step LEI was measured herein to be a factor of 30 and 600, respectively, as the configurations of two beams were changed to propagate in the opposite direction along the burner slot. The only restriction for this version is to assume validity of the steady-state approximation for the first-step intermediate state and a local thermal equilibrium in the flame. In the LEI scheme, a weak excitation rate is

applied, and subsequently the excited population is removed rapidly due to a relatively large ionization rate. This observation suggests that the steady-state approximation should be applicable to the system.[13,28,30] The assumption of a thermally equilibrated flame is the premise for those detection methods applying Boltzmann distribution.

*Temperature by Other Optical Methods.* To justify the reliability of our LEI measurement, we compared the measured temperature in an atmospheric air/acetylene flame with various optical methods. These methods include atomic absorption (AA),[31,32] atomic emission (AE),[31,33] atomic fluorescence (AF),[34–36] and the LEI measurement[26] reported previously. Although different ratios of air to acetylene have been adopted, one finds that the resultant temperatures tend to decrease in a fuel-rich flame. Using the AF method, for instance, Haraguchi and Winefordner reported a temperature of 2400 K with an air/fuel ratio of 7.6:1.04 at a 3 mm height above the burner head.[36] In terms of AA measurement, Browner and Winefordner gave a value of 2450 K with the ratio of 9.5:1.3 at a 4.5 mm height.[32] With the AE method, Kirkbright et al. obtained a result of 2420 K with the ratio of 10.0:1.35 at the 4.5 mm height.[33] With the use of AA coupled to fiber-optics detection, Wang et al. reported a lower temperature of 1910–2230 K at a height range of 5–30 mm in an even more fuel-rich flame, into which the flow rates of air and acetylene were 6.7 and 1.7 L/min.[37] The latter discrepancy may arise from the presence of more carbon-containing radicals; incomplete reaction may lower the resulting temperature. In contrast, the previous LEI measurement exhibited a slightly higher temperature of 2504–2521 K in a fuel-leaner flame, composed of an air/fuel ratio of 12.5:0.5 at 7.5 mm from the burner top.[26] The combustion thus obtained was more complete. Fernandez and Bastiaans have demonstrated the stoichiometry effect on the flame temperature in the central portion, 11 cm above the top of a premixed Meker-type burner.[38] They found that the temperature tended to increase to a maximum with an increase in the ratio of air to acetylene. The tendency is essentially consistent with the stoichiometry dependence found in a rectangular burner.

*Radial and Axial Temperature Profiles.* The present work yields a spatially resolved temperature, which greatly reduces the interference of thermal gradients and is not limited to observation of an averaged temperature along the laser-beam path. The temperatures 2550 and 2440 K were measured in the central and the edge regions, respectively. The radial distribution is roughly symmetric. The average temperature, as evaluated by summing each point-temperature along the axis of the burner slot, is consistent with that determined by old LEI method.[26] The lower temperature in the edge found by Fernandez and Bastiaans was in a cylindrical flame,[38] and that detected by Wang et al. was in a slot burner.[37] The entrainment of external air renders the flame subject to change in local stoichiometry, which decreases the temperature. The precision of temperature evaluated in the edge appears to be poor relative to the central portion, since flame instability reduces the signal-to-noise ratio. In this work, the axial flame distribution reveals that the temperature decreases slightly with height from the burner top. The tendency is consistent with the reports by Kirkbright et al. with a home-made slot burner,[39] and by Eckbreth using the CARS technique to probe a laminar propane diffusion flame.[40] In contrast, Wang et al. showed an opposite tendency in a very fuel-rich flame.[37]

*RID versus LEI.* In contrast to our excitation temperature measurement, Winefordner and co-workers recently determined a spatially resolved OH rotational temperature using indium-based resonance ionization detection (RID).[41,42] The RID technique is similar to the two-step LEI detection as described herein. However, the first-step population excitation in the RID detection is achieved through two mechanisms, collision-induced energy transfer and fluorescence capture.[41] The ionization detector thus has the advantages of the LEI method, including a relatively large solid angle of signal collection, a near-unity quantum efficiency, and the minimization of optical interference. The application of RID detection to the OH rotational temperature did improve the detection sensitivity and selectivity.[42] However, the following restriction seems to be imposed on the RID method; the rates of collisional energy transfer and the excitation transition probabilities induced by fluorescence capture are assumed to be independent of the flame species and the rotational quantum states of the OH radical. The RID temperature may then be derived, on the basis of theoretical modeling that is well developed for the fluorescence or emission methods. The above assumption complicates the RID method. The complexity of such indirect processes involved as the first-step excitation in the RID scheme might be the factor leading to an unexpectedly higher temperature occurring in the flame edge.[42] It might also explain, alternatively, the appearance of a relatively poor precision as compared with that for the LIF method.

## CONCLUSION

The two-step LEI method has been shown to be potentially useful in measuring spatially resolved excitation temperatures in an atmospheric air/acetylene flame. Given the ratio of two-step LEI signal and its corresponding laser energy associated with the fine-structure doublets of the species selected, the flame temperature may be determined. This approach provides a convenient and accurate measurement without the need to know the absolute beam energy and to calibrate the detection system. The accuracy and precision for the measured temperature profiles in terms of Al and Ga species are comparable with those by other optical methods.


### ACKNOWLEDGMENT

This work was financially supported by the National Science Council of the Republic of China under Contract No. NSC86-2113-M002-038.



1. A. G. Gaydon and H. G. Wolfhand, *Flames: Their Structure, Radiation and Temperature* (Chapman and Hall, London, 1979), 4th ed.
2. C. Th. J. Alkemade, T. Hollander, W. Snelleman, and P. J. Th. Zeegers, *Metal Vapors in Flames* (Pergamon Press, New York, 1982).
3. A. C. Eckbreth, *Laser Diagnostics for Combustion Temperature and Species* (Abacus Press, Cambridge, 1988).
4. J. D. Bradshaw, N. Omenetto, G. Zizak, J. N. Bower, and J. D. Winefordner, Appl. Opt. **19,** 2709 (1980).
5. R. G. Joklik, Combust. Sci. and Tech. **87,** 109 (1992).

6. N. Omenetto, R. Browner, J. D. Winefordner, G. Rossi, and P. Benetti, Anal. Chem. **44,** 1683 (1972).
7. D. R. Crosley, *Laser Probes for Combustion Chemistry,* ACS Symp. Ser. No. 134 (American Chemical Society, Washington, D.C., 1980).
8. P. Ewart, Ber. Bunsenges. Phys. Chem. **97,** 1625 (1993).
9. T. Dreier and D. J. Rakestraw, Opt. Lett. **15,** 72 (1990).
10. D. Kupiszewska and B. Whitaker, J. Chem. Soc. Faraday Trans. **89,** 2951 (1993).
11. J. C. Travis, G. C. Turk, and R. B. Green, Anal. Chem. **54,** 1006A (1982).
12. O. Axner, I. Lindgren, I. Magnusson, and H. Rubinsztein-Dunlop, Anal. Chem. **57,** 773 (1985).
13. N. Omenetto, Th. Berthoud, P. Cavalli, and G. Rossi, Anal. Chem. **57,** 1256 (1985).
14. C. A. van Jijk, F. M. Curran, K. C. Lin, and S. R. Crouch, Anal. Chem. **53,** 1275 (1981).
15. K. D. Su and K. C. Lin, Appl. Spectrosc. **48,** 241 (1994).
16. G. C. Turk, Anal. Chem. **53,** 1187 (1981).
17. K. D. Su, K. C. Lin, and W. T. Luh, Appl. Spectrosc. **42,** 1370 (1992).
18. G. C. Turk and N. Omenetto, Appl. Spectrosc. **40,** 1085 (1986).
19. E. G. Mallard and K. C. Smyth, Comb. Flame **44,** 61 (1982).
20. K. C. Lin, P. M. Hunt, and S. R. Crouch, Chem. Phys. Lett. **90,** 111 (1982).
21. T. A. Cool and P. J. H. Tjossem, in *Gas-Phase Chemiluminescence and Chemi-ionization,* A. Fontijn, Ed. (Elsevier Science Publishers, Amsterdam, 1985), pp. 105–116.
22. S. C. Wang and K. C. Lin, Anal. Chem. **66,** 2180 (1994).
23. S. C. Wang and K. C. Lin, Analyst **120,** 2593 (1995).
24. T. Berglind, S. Nillson, and H. Rubinstein-Dunlop, Phys. Scripta **36,** 246 (1987).
25. K. S. Epler, T. C. O'Haver, G. C. Turk, and W. A. MacCreham, Anal. Chem. **60,** 2062 (1988).
26. K. D. Su, C. Y. Chen, K. C. Lin, and W. T. Luh, Appl. Spectrosc. **41,** 1340 (1991).
27. O. Axner and S. Sjostrom, Appl. Spectrosc. **44,** 864 (1990).
28. J. C. Travis, J. Chem. Educ. **59,** 909 (1982).
29. O. Axner, M. Norberg, and H. Rubinsztein-Dunlop, Spectrochim. Acta **44B,** 693 (1989).
30. L. Volk, W. Richardson, K. H. Lau, M. Hall, and S. H. Lin, J. Chem. Educ. **54,** 95 (1977).
31. L. De Galan and G. F. Samaey, Spectrochim. Acta **25B,** 245 (1970).
32. R. F. Browner and J. D. Winefordner, Anal. Chem. **44,** 247 (1972).
33. G. F. Kirkbright, M. Sargent, and S. Vetler, Spectrochim. Acta **25B,** 465 (1970).
34. M. Omenetto, D. Benetti, and G. Rossi, Spectrochim. Acta **27B,** 453 (1972).
35. H. Haraguchi, B. Smith, S. Weeks, D. J. Johnson, and J. D. Winefordner, Appl. Spectrosc. **31,** 156 (1977).
36. H. Haraguchi and J. D. Winefordner, Appl. Spectrosc. **31,** 195 (1977).
37. J. Wang, S. Li, X. Wang, W. Li, Z. Chen, and Y. Luo, Spectrosc. Lett. **25,** 769 (1992).
38. M. A. Fernandez and G. J. Bastiaans, Appl. Spectrosc. **33,** 145 (1979).
39. G. F. Kirkbright, M. K. Peters, M. Sargent, and T. S. West, Talanta **15,** 663 (1968).
40. A. C. Eckbreth, in *Laser Probes for Combustion Chemistry,* D. R. Crosley, Ed. ACS Symp. Ser. No. 134 (American Chemical Society, Washington, D.C., 1980), pp. 271–301.
41. G. A. Petrucci, D. Imbroisi, B. W. Smith, and J. D. Winefordner, Spectrochim. Acta **49B,** 1569 (1994).
42. G. A. Petrucci, D. Imbroisi, R. D. Guenard, B. W. Smith, and J. D. Winefordner, Appl. Spectrosc. **49,** 655 (1995).
43. W. L. Wiese and G. A. Martin, *Wavelengths and Transition Probabilities for Atoms and Atom Ions,* Part II, NSRDS-NBS 68 (U.S. Government Printing Office, Washington, D.C., 1980).